Probing CdS Nanocrystal Surfaces with Laser-Polarized Xenon

C. R. Bowers,*,† T. Pietrass, E. Barash, A. Pines, R. K. Grubbs, and A. P. Alivisatos

Materials Sciences Division, Lawrence Berkeley Laboratory, 1 Cyclotron Road, Berkeley, California 94720, and Department of Chemistry, University of California, Berkeley, California 94720

Received: July 22, 1994[⊗]

This paper describes the application of optically pumped xenon NMR to probe the surface of semiconductor nanocrystals by physisorption at 123 K. These experiments were made possible by using highly spin ordered ^{129}Xe, prepared by optical pumping and spin exchange of a rubidium xenon gas mixture, to increase the NMR signal strength. CdS nanocrystals were prepared by regulated growth in inverse micelles and precipitated by surface derivatization with thiophenol. Nanocrystals of 11.8, 12.8, and 23 Å radii with 26%, 63%, and 57% thiophenol surface coverage, respectively, were characterized. Within this sample parameter space, the ^{129}Xe spectra, recorded at varying xenon coverages, depended strongly on thiophenol surface coverage but were not sensitive to the crystallite size. In addition, the nanocrystals with low thiophenol coverage yielded a xenon line shape consisting of two components, interpreted as xenon signals arising from distinct surface domains. These domains are presumably formed by the aggregation of thiophenol molecules on the nanocrystal surface when the thiophenol coverage is incomplete, a model which is consistent with existing X-ray photoelectron spectroscopy and liquid state ^1H NMR data.

In the past few years, new synthetic methods have been developed to prepare macroscopic quantities of semiconductor nanocrystals with diameters ranging from 10 to 100 Å, a size regime in which quantum dot behavior is evident. A high degree of monodispersity in size, shape, and crystallinity is afforded by these new chemical methods. These qualities are essential for the interpretation of spectroscopic data pertaining to the structure and dynamics in these quantum confined systems.

A key step in the synthetic methods for the preparation and isolation of stable CdS and CdSe nanocrystal samples is the chemical passivation of the surface. Crystallite termination plays an integral role in the excitonic trapping and recombination processes.[1] The surface atoms in crystallites of such small dimensions can comprise a substantial fraction of the particle: for example, about one-third of the atoms of a 26 Å diameter nanocrystal reside at the surface. This motivates an investigation of the composition and morphological parameters which characterize the surface derivatization, such as the fractional coverage and spatial distribution of the passivating groups. Fractional coverages by thiophenol or phosphine oxide capped CdS and CdSe nanocrystals have recently been determined by liquid state ^1H NMR,[2] X-ray photoelectron[3] spectroscopy (XPS), and phosphorus NMR.[4] In the thiophenol capped CdS nanocrystals, the ^1H NMR T_2 measurements along with relaxation modeling suggest that the bonding to the thiophenol sulfur atom is in the terminal rather than in the bridging geometry and that the molecules aggregate to form "islands" when the surface coverage is not complete.[2] The latter issue is of particular interest in the present work.

NMR is well suited for the study of semiconductor nanocrystals. It is element selective and can quantify both chemical composition and local electronic structure in the absence of long-range order. In addition to the thiophenol ^1H relaxation work noted above, several other NMR studies of the nanocrystal system have also appeared in the literature. Solid state magic angle spinning NMR has been applied to the CdS nanocrystal systems to study the bonding environment of surface and core atoms.[5] Using liquid state ^{77}Se NMR, Duncan et al. attributed the shifts and broadenings of the resonance they observed to the effect of quantum confinement on the average excitation energy in the paramagnetic term of Ramsey's chemical shift theory.[6]

The study of the nanocrystal surface structure requires a spectroscopic method that (a) can differentiate between the surface and interior sites and (b) provides information about local order in the absence of long-range order. While conventional NMR can provide capping group coverages and XPS can completely determine the surface composition, neither method can be used to directly characterize the overall surface structure or morphology. Clearly, the thiophenol distribution will be determined by three primary factors: the distribution of surface cadmium atoms, attractive interactions between the thiophenol groups, and steric effects. Given that the lattice of the nanocrystal core is known to be zinc blende in particles formed in inverse micelles,[5] two distinct models for the surface structure can be proposed, representing the extremes in a continuum of possible arrangements. The first model propounds the existence of a particle boundary defined by facet planes, consisting of either cadmium, sulfur, or both cadmium and sulfur. Since thiophenol is known to bond exclusively with cadmium on the nanocrystal surface, facet formation naturally leads to two distinct domain types: those covered by thiophenol and those not. In this case the distribution of thiophenol is entirely governed by the distribution of surface cadmium atoms. In the second model, the particle shape more closely approximates that of a sphere, yielding a more uniform distribution of cadmium. Attractive forces between thiophenol molecules on the cluster surface would then be responsible for the formation of thiophenol islands or aggregates.

How, then, can the factors governing the spatial distribution of capping groups, such as the occurrence of facet planes or cavities, intermolecular forces, and surface reconstruction, be elucidated? In this study, the question of surface morphology will be addressed by the interpretation of the NMR spectra of ^{129}Xe physisorbed to the surface of thiophenol capped nano-

* To whom correspondence should be addressed.
† Present address: Chemistry Department, University of Florida, Gainesville, Florida 32611.
⊗ Abstract published in *Advance ACS Abstracts,* September 1, 1994.

0022-3654/94/2098-9400$04.50/0

crystals of varying size and thiophenol coverage. Physisorbed ^{129}Xe has the advantage of being a surface selective probe and of exhibiting an enormous chemical shift range that serves as a highly sensitive indicator of its local electronic environment. For this reason, conventional ^{129}Xe NMR has been widely used in the characterization of microporous solids, such as zeolites,[8] supported metal particles,[9] and occluded materials such as clathrates.[10] Disadvantageously, however, the low NMR detection sensitivity of ^{129}Xe usually precludes its application at moderate temperatures for all samples except those with high surface area (>100 m^2/g) and short xenon relaxation times, T_1 < 1 s. Here, this limitation was circumvented by applying the method of optical pumping and spin exchange, in which nearly complete nuclear spin ordering of the xenon can be achieved by angular momentum transfer from circularly polarized laser photons. In comparison, recall that in conventional NMR immersion of the sample in a magnetic field produces a Curie law polarization of merely a few parts per million. In practice, optical pumping and spin exchange can improve the detection sensitivity by as much as 4−5 orders of magnitude over conventional NMR.

Laser-polarized xenon has previously been used to improve the sensitivity of the NMR of xenon in dynamic equilibrium with the surface of semicrystalline polymers[11] and other materials with relatively low surface areas of <10 m^2/g.[12] Cross-polarization, an extension of this technique wherein nuclear spin polarization is transferred from the xenon to the spins comprising the material of interest, has also been achieved from ^{129}Xe to ^{131}Xe,[13] to ^{13}C in Xe−$^{13}CO_2$ mixtures,[14] and to ^1H nuclei in poly(triarylcarbinol),[15] a highly cross-linked, microporous polymer. In this laboratory, experimental developments involving cross-polarization from laser-polarized xenon to other materials, including the semiconductor nanocrystal system, are currently in progress in an effort to generalize the applicability of this technique. However, the primary objective of the present work is to evaluate the sensitivity of optically pumped xenon NMR to the general problem of surface composition and derivatization of nanocrystal materials.

Highly polarized ^{129}Xe was prepared by gas phase spin exchange with optically pumped rubidium. The physics of this process is described in detail elsewhere.[16] In a typical run, 200 Torr of xenon gas, enriched to 80% in the ^{129}Xe isotope and depleted to 1.3% in ^{131}Xe, was combined with rubidium vapor at a temperature of 350 K and irradiated on resonance with the ^{87}Rb and ^{85}Rb ^1D lines for 30 min with 1−1.5 W of circularly polarized light. The source of the optical pumping field was an argon ion pumped CW titanium sapphire ring laser with an optical line width of about 10 MHz. A $\lambda/4$ plate and a lens were used to circularly polarize the beam and expand it so as to illuminate the entire 35 cm^3 pumping cell. The $\bar{k}$ vector of the light was directed coaxially with the 50 G fringe field directly beneath the bore of the 4.2 T superconducting NMR magnet, where the optical pumping cell was located. The xenon polarization was estimated to be on the order of 10−20%. The ^{129}Xe Larmor frequency at high field was 49.45 MHz.

CdS nanocrystals were prepared via an inverse micelle method developed by Steigerwald et al.[17] and Lianos et al.[18] In a typical synthesis, two separate solutions were prepared, each containing 44.4 g of dioctyl sulfosuccinate (AOT) dissolved in 500 mL of spectrographic grade heptane. The solutions were deoxygenated with nitrogen gas for 1 h. Into the first heptane solution was added 0.84 g of $Cd(ClO_4)_2 \cdot 6H_2O$ in 13.0 mL of deoxygenated and deionized water. A solution containing 0.26 g of $Na_2S \cdot 9H_2O$ in 13.0 mL of deoxygenated and deionized water was added to the second heptane solution. The cadmium/heptane solution was then slowly added to the sulfide/heptane solution with vigorous stirring under gaseous nitrogen, yielding a clear yellow solution. Upon addition of 0.3 mL of thiophenol, the solution turned cloudy as the CdS nanocrystals precipitated. Vacuum filtration followed by repeated washings with petroleum ether yielded nanocrystals of poor quality. A final dissolution in pyridine (or ethylpyridine) followed by reprecipitation in petroleum ether, filtration, and thorough washing with petroleum ether is necessary to obtain high-quality CdS nanocrystals as verified by solution state ^1H NMR and UV−vis absorption spectroscopies.

TABLE 1

sample	radius (Å)	no. of thiophenols per nanocrystal	coverage (%)
1	12.8 ± 0.5	37−40	26−27
2	11.8 ± 0.5	90−95	63−64
3	23.0 ± 1.5	286−357	55−59

The samples were stored under nitrogen and refrigerated until used in the xenon NMR experiments, which were performed within 2 weeks of sample preparation. Nanocrystal radii were determined from measurements of the band gap by optical absorption spectra and its known dependence on nanocrystal size as determined from TEM images and powder X-ray diffraction.[7,19] The number of atoms in the crystallite was then determined using the bulk density of CdS since the lattice spacing is the same as in the nanocrystals.[7] Hence, given a crystallite radius r and unit cell lattice constant a, the total number of atoms per nanocrystal is given by

$$N = \frac{4\pi}{3}\left(\frac{2r}{a}\right)^{1/3}$$

The number of surface atoms was then calculated by subtracting from N the number of atoms in a particle smaller in radius by the Cd−S bond length of 2.52 Å.[20] The number of thiophenol molecules per crystallite was determined by liquid state ^1H NMR, using a weighed quantity of methylene chloride added to the fully deuterated pyridine solvent as an internal intensity reference. The fractional coverage is given by the ratio of thiophenol molecules to the number of surface atoms (Cd + S). The characteristics of the three different nanocrystal samples studied are summarized in Table 1. These characteristics were chosen in order to critically evaluate the sensitivity of the xenon NMR to nanocrystal size and thiophenol coverage. Variation of the surface thiophenol coverage was achieved in the synthesis by varying the number of thiophenol reagent molecules with respect to the number of surface atoms present in the unterminated particle, with the latter being determined by the surfactant to solvent proportions. Since thiophenol binds only to cadmium, the reported coverages exceeding 50% require an excess of cadmium to be present in the surface layer. Coverages exceeding 50% have also been observed in phosphine oxide capped CdSe nanocrystals.[3]

The thick-walled pyrex glass sample holder, which is similar to the one described in ref 11 except that it was "L"-shaped, was packed with ~150 mg of CdS nanocrystals and evacuated for >8 h at a vacuum of 10^{-5} Torr or lower prior to the xenon adsorption experiments. All experiments described herein were conducted at a sample temperature of 123 ± 3 K, maintained by flowing N_2 gas through the dewared probe-head region. Once the xenon gas obtained its maximum attainable polarization, the optical pumping cell was cooled to room temperature, allowing the xenon gas to be separated from the condensed rubidium metal. The xenon was then introduced to the sample by opening a stopcock to the sample region. After allowing 10 s for equilibration, the xenon free induction decay was

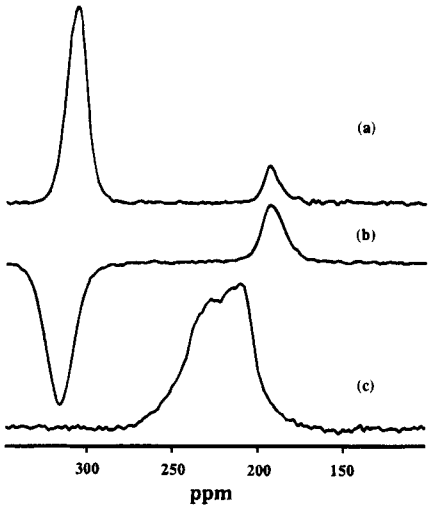

Figure 1. Laser-enhanced NMR spectra of ^{129}Xe physisorbed at 123 K onto CdS nanocrystal samples. (a) Sample 3, r = 23 Å, high thiophenol coverage. The peak at 310 ppm is the signal due to bulk solid xenon. (b) Sample 2, r = 11.8 Å, high thiophenol coverage. The solid xenon peak is inverted due to storage along the $-z$ axis by a previous pulse. (c) Sample 1, r = 12.8 Å, low thiophenol coverage.

stimulated by a single radio-frequency pulse or with a $90-\tau-180-\tau$ echo sequence. The initial and final pressures of the xenon gas were recorded, permitting samples to be compared on the basis of their xenon NMR line shapes as well as the dependence of the spectra on the number of moles of added xenon.

The laser-enhanced ^{129}Xe spectra for all three samples with the same mass of xenon added are shown in Figure 1a–c. Samples 2 and 3, which are similar with respect to thiophenol coverage but differ substantially in size, exhibit nearly identical xenon NMR spectra. A single broad physisorbed xenon peak occurs at about 190 ppm along with a strong signal corresponding to bulk xenon at 320 ppm. (The solid xenon peak is inverted in (b) due to magnetization stored along the $-z$ axis by a previous pulse, an effect which has no consequence on the adsorbed xenon peak on account of its relatively short T_1.) By comparison, a markedly different xenon spectrum is obtained with the same amount of xenon added to sample 1. This sample yields an NMR line shape which can be decomposed into a sum of two Lorentzian peaks with areas in the ratio of 2:1. These contrasting xenon NMR signatures are also evident in the observed chemical shift dependences on the molar quantity of xenon added to the samples, as shown in Figure 2a–c. For samples 2 and 3, those with high thiophenol coverage, the shift sharply rises but then saturates at about 200 ppm, at which point a strong xenon signal corresponding to solid xenon appears. Sample 1, with partial thiophenol coverage, yields two resonances which progressively shift to lower field with added xenon, far beyond the 200 ppm saturation point for the other samples. The spectra at three different values of the adsorbed xenon volume V_{ads} are shown in Figure 3a–c. For all xenon coverages, the line shape can be fit to a sum of two Lorentzians with areas in the ratio of 2:1, a ratio which does not substantially vary with the amount of xenon adsorbed onto the nanocrystal surface. Notice also that the line width of each component narrows with increasing xenon coverage, as plotted in Figure 4. This is probably indicative of the more homogeneous electronic environment surrounding the xenon nucleus at higher xenon coverages.

The observation of two distinct resonances indicates that the xenon experiences two different electronic environments that are spatially separated to such an extent that the xenon cannot

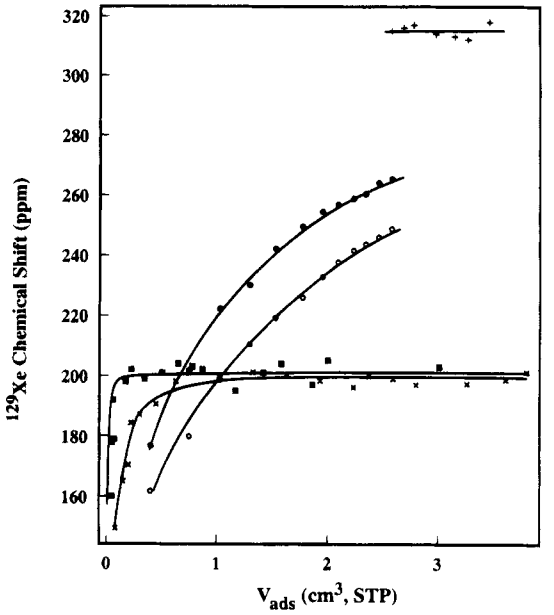

Figure 2. Dependence of the ^{129}Xe chemical shift on the adsorbed volume of xenon for three different CdS nanocrystal samples. Legend for curves is as follows: filled and open circles, sample 1, components 1 and 2; crosses, sample 2; filled squares, sample 3; pluses, bulk solid xenon. Sample characteristics are given in Table 1.

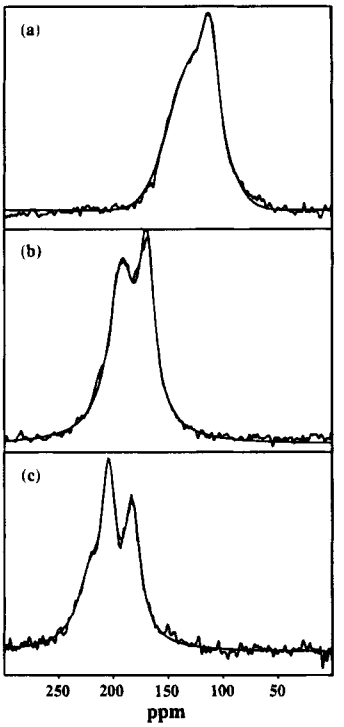

Figure 3. NMR spectra of ^{129}Xe physisorbed onto sample 1 (r = 12.8 Å) with a surface thiophenol coverage of 26%. The sensitivity was enhanced by optical pumping and spin exchange, as described in the text. The spectra were recorded at a temperature of 123 K, with the following xenon coverages: (a) V_{ads} = 0.4 cm^3 (STP), 0.2 monolayers; (b) 0.76 monolayer, (c) 1.0 monolayer. Also shown is the fit of each spectrum to a sum of two Lorentzians.

rapidly diffuse between those environments. Rapid exchange would yield a single peak occurring at the weighted average of the chemical shifts associated with each environment. The observed spectral features for sample 1 can be explained by the existence of surface domains, formed by the aggregation of thiophenol molecules on the nanocrystal surface when the thiophenol coverage is incomplete. Each domain is associated with an electronic environment yielding a unique xenon

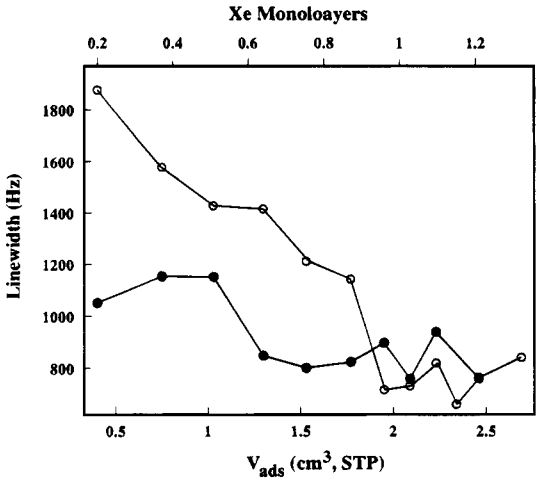

Figure 4. ^{129}Xe NMR line width of the downfield (open circles) and upfield (solid circles) spectra components decreases as a function of the xenon physisorption for sample 1, $T = 123$ K. The ^{129}Xe Larmor frequency is 49.45 MHz.

chemical shift. *Note that this line shape was not effected by macroscopic grinding or packing of the sample.* In a separate experiment, two well-resolved physisorbed ^{129}Xe signals were also observed in phenylselenol capped cadmium selenide nanocrystals.

The occurrence of discrete surface domains can be probed by the NMR of physisorbed ^{129}Xe provided that the domains cause different chemical shifts. The two-dimensional random walk of a xenon atom on a surface leads to a mean-squared displacement which is given by $\langle(\Delta\vec{r})^2\rangle = 4D^*t$, where $D^* = D_0e^{-E_{diff}/(kT)}$ and E_{diff} characterizes the height of the lateral diffusion barrier. A rate for exchange between domains can be estimated by solving for $1/t$ with the mean-squared displacement equated with the center-to-center domain separation, $\langle(\Delta\vec{r})^2\rangle = \langle d^2\rangle$. When the domain size is large enough and the diffusion coefficient small enough so that xenon cannot physically exchange between the domains on the time scale of the inverse chemical shift difference, the chemical shifts may be resolved in the spectrum. This is roughly expressed by the condition

$$4D^*/\langle d^2\rangle \leq \omega_1 - \omega_2$$

where ω_1 and ω_2 are the chemical shifts (in rad/s) of the xenon physisorbed onto domain types 1 and 2. If a maximum domain separation of half the particle circumference is assumed, an upper bound on D^* and consequently E_{diff} can be determined. From the spectra, the chemical shift difference is $\omega_1 - \omega_2 = 6200$ rad/s. Letting $\langle d^2\rangle \sim (12.8 \times 10^{-8}\pi)^2$ yields $D^* \leq 2.5 \times 10^{-10}$ cm^2/s. For comparison, the diffusion coefficient at saturation coverage of xenon on a Pt(111) surface is $D^* = 2 \times 10^{-8}$ cm^2/s at 80 K.[21] If a value for the preexponential diffusion coefficient of $D_0 \approx 4 \times 10^{-4}$ cm^2 for xenon on a Pt(111) surface[21] is assumed, E_{diff} is estimated to be on the order of 3.5 kcal/mol. For comparison, E_{diff} at saturation coverage on a Pt-(111) surface has been measured to be 1.3 kcal/mol. Since the electron density at the surface of a metallic single crystal surface is expected to be considerably more uniform than that of the capped nanocrystal surface, the estimate for E_{diff} is not qualitatively unreasonable. A measure of the lateral adsorbate–surface potential relative to the adsorption energy of the system is given by the corrugation ratio, defined as $\Omega = E_{diff}/\Delta E_{ads}$. From the xenon adsorption isotherms, the enthalpy of xenon adsorption onto the 12.8 Å sample was found to be 4.6 kcal/mol at $T = 140$ K, yielding $\Omega = 0.75$.

To summarize, a study of CdS nanocrystal surfaces has been accomplished by using laser-polarized ^{129}Xe and NMR. This is clearly a case where the method of optical pumping and spin exchange has extended the applicability of ^{129}Xe NMR to a surface upon which the xenon T_1 would have been prohibitively long for conventional NMR. The ^{129}Xe NMR line shape and its dependence on xenon coverage are highly sensitive to the variation of the surface derivatization, but a size dependence of the shift or line shape was not observed. The xenon NMR is insensitive to differences in the nanocrystal size over the range of $r = 11.8$ to $r = 23$ Å in the regime of high thiophenol coverage. The observation of two resonances in the particles with only 26% thiophenol coverage appears indicative of surface domains. One possibility is that domains are formed by the aggregation of thiophenol molecules, as was first suggested in ref 2. Such domain formation could be explained by the existence of facet planes containing predominantly cadmium or sulfur, since thiophenol is known to bond only with cadmium. This model can be ruled out because it would predict the observation of two peaks in the spectrum even at high thiophenol coverage. Alternatively, the observations are consistent with domain formation due to intermolecular thiophenol interactions on particles roughly spherical in shape and uniform in the distribution of surface cadmium atoms. The integrated intensities of these resonances are in the ratio of 2:1 which correlates stoichiometrically with the fractional thiophenol coverage of 26%. Interpretation of the spectra in terms of a domain model leads to an upper bound for D^*, an estimate for the lateral diffusion barrier E_{diff}, and when combined with the measured adsorption energy, a value for the corrugation ratio of the surface. However, another possibility that cannot be ruled out is the existence of cavities, i.e., a microporous surface morphology that allows xenon to penetrate into the surface of the particle.

Experiments are planned to measure the diffusion coefficient D^* directly, using either radio-frequency hole-burning techniques or two-dimensional ^{129}Xe exchange NMR,[22,23] to further test the validity of the thiophenol island model and allow a quantitative determination of the domain size. Future efforts to investigate the nanocrystal surfaces with laser polarized xenon will extend the data set of this study to a finer variation in the thiophenol coverages and particle sizes, as well as to nanocrystal systems with other capping groups, such as phosphine oxide. Experiments involving the cross-polarization from laser-polarized ^{129}Xe to surface ^{1}H, ^{113}Cd, or ^{77}Se nuclei are also under way. These experiments will yield quantitative information about surface defects and the bonding geometries due to surface reconstruction.

Acknowledgment. This work was funded by the Director, Office of Energy Research, Office of Basic Energy Sciences, Materials Sciences Division, U.S. Department of Energy, under Contract DE-AC0376SF0098. Support from the Shell Development Co. is also acknowledged. T.P. acknowledges support by the NATO–DAAD postdoctoral fellowship program. Thanks to L. Reven for construction of the xenon optical pumping probe and to H. Long for construction of the optical pumping cell. Useful discussion with J. E. Bowen-Katari, V. L. Colvin, J. J. Shiang, and S. H. Tolbert are gratefully acknowledged.

References and Notes

(1) Bawendi, M. G.; Carroll, P. J.; Wilson, W. L.; Brus, L. E. *J. Chem. Phys.* **1992**, *96*, 946.

(2) Sachleben, J. R.; Wooten, E. W.; Emsley, L.; Pines, A.; Colvin, V. L.; Alivisatos, A. P. *Chem. Phys. Lett.* **1992**, *198*, 431.

(3) Bowen Katari, J. E.; Colven, V. L.; Goldstein, A. N.; Tu, A.; Alivisatos, A. P. *J. Phys. Chem.*, submitted for publication.

(4) Bawendi, M. G.; Griffin, R. G. *J. Chem. Phys.* **1994**, *100*, 3297.
(5) Herron, N.; Wang, Y.; Eckert, H. *J. Am. Chem. Soc.* **1993**, *112*, 1322.
(6) Thayer, A. M.; Steigerwald, M. L.; Duncan, T. M.; Douglass, D. C. *Phys. Rev. Lett.* **1988**, *60*, 2673.
(7) Murray, C. B.; Norris, D. J.; Bawendi, M. G. *J. Am. Chem. Soc.* **1993**, *115*, 8703.
(8) (a) Springuel-Huet, M. A.; Fraissard, J. *Chem. Phys. Lett.* **1989**, *154*, 299. (b) Ito, T.; Fraissard, J. *Zeolites* **1988**, *8*, 350. (c) Davis, M. E.; Saldarriaga, C.; Montes, C.; Hanson, B. *J. Chem. Phys.* **1988**, *92*, 2557. (d) Chmelka, B. F.; de Menorval, L. C.; Csencsits, R.; Ryoo, R.; Liu, S.-B.; Radke, C. J.; Petersen, E. E.; Pines, A. In *Structure and Reactivities of Surfaces*; Morterra, C., et al., Eds.; Elsevier: Amsterdam, 1989; p 269. (e) Chmelka, B. F.; Pearson, J. G.; Liu, S.-B.; Ryoo, R.; de Menorval, L. C.; Pines, A. *J. Phys. Chem.* **1991**, *95*, 303.
(9) Davidson, D. W.; Handa, Y. P.; Ripmeester, J. A. *J. Phys. Chem.* **1986**, *90*, 6549.
(10) Ripmeester, J. A.; Ratcliffe, C. I.; Tse, J. S. *J. Chem. Soc., Faraday Trans. 1* **1988**, *84*, 3731.
(11) Raftery, D.; Reven, L.; Long, H.; Pines, A.; Tang, P.; Reimer, J. A. *J. Phys. Chem.* **1993**, *97*, 1649.
(12) Raftery, D.; Long, H.; Meersmann, T.; Grandinetti, P. J.; Reven, L.; Pines, A. *Phys. Rev. Lett.* **1991**, *66*, 584.
(13) Cates, G. D.; Benton, D. R.; Gatzke, M.; Happer, W.; Hasson, K. C.; Newbury, N. R. *Phys. Rev. Lett.* **1990**, *65*, 2591.
(14) Bowers, C. R.; Long, H. W.; Pietrass, T.; Gaede, H. C.; Pines, A. *Chem. Phys. Lett.* **1993**, *205*, 168.
(15) Long, H. W.; Gaede, H. C.; Shore, J.; Reven, L.; Bowers, C. R.; Kritzenberger, J.; Pietrass, T.; Pines, A. *J. Am. Chem. Soc.* **1993**, *115*, 8491.
(16) (a) Kastler, A. *J. Phys. Radium* **1950**, *11*, 255. (b) Bouchiat, M. A.; Carver, T. R.; Varnum, C. N. *Phys. Rev. Lett.* **1960**, *5*, 373. (c) Bhaskar, N. D.; Happer, W.; Larsson, M.; Zeng, X. *Phys. Rev. Lett.* **1983**, *50*, 105.
(17) Steigerwald, M. L.; Alivisatos, A. P.; Gibson, J. M.; Harris, T. D.; Kortan, R.; Muller, A. J.; Thayer, A. M.; Duncan, T. M.; Duncan, T. M.; Douglas, D. C.; Brus, L. E. *J. Am. Chem. Soc.* **1988**, *110*, 3046.
(18) Lianos, P.; Thomas, J. K. *Chem. Phys. Lett.* **1986**, *125*, 299.
(19) Lippens, P. E.; Lannoo, M. *Phys. Rev. B* **1989**, *39*, 10935.
(20) Wyckoff, R. W. G. *Crystal Structures*, 2nd ed.; Interscience Publishers: New York, 1963.
(21) Meixner, D. L.; George, S. M. *J. Chem. Phys.* **1993**, *98*, 9115.
(22) Jeener, J.; Meier, B. H.; Bachmann, P.; Ernst, R. R. *J. Chem. Phys.* **1979**, *71*, 4546.
(23) Meier, B. H.; Ernst, R. R. *J. Am. Chem. Soc.* **1979**, *101*, 6441.